AD-A141 552 INVESTIGATION OF THE DETECTABILITY AND LIFETIME OF GUST FRONTS AND OTHER..(U) NATIONAL OCEANIC AND ATMOSPHERIC ADMINISTRATION NORMAN OK NAT.. D S ZRNIC ET AL. OCT 83 1/1

UNCLASSIFIED DOT/FAA/PM-83/33 DTFA01-81-Y-10521 F/G 4/2 NL

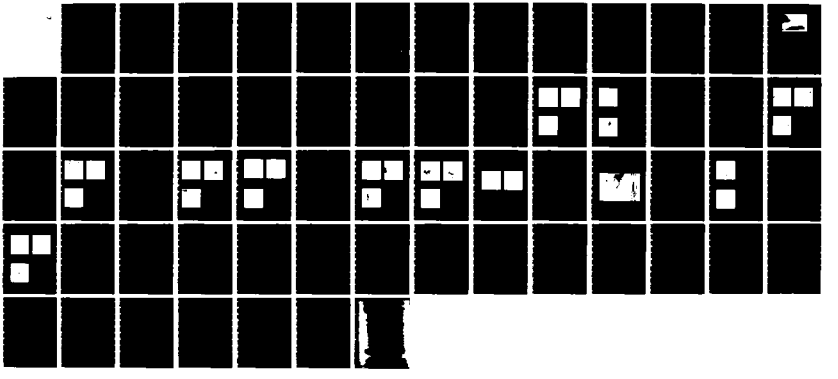

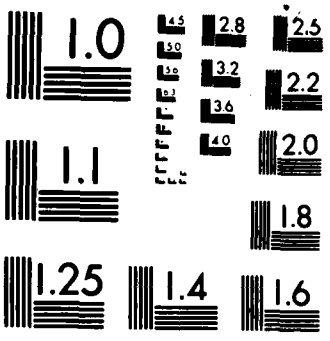

DOT/FAA/PM-83/33

Program Engineering &
Maintenance Service
Washington, D.C. 20591

Investigation of the Detectability and Lifetime of Gust Fronts and Other Weather Hazards to Aircraft

Dusan S. Zrnic'
Jean T. Lee

October 1983

Final Report

U.S. Department of Transportation
Federal Aviation Administration

NOTICE

This document is disseminated under the sponsorship of the Department of Transportation in the interest of information exchange. The United States Government assumes no liability for its contents or use thereof.

Technical Report Documentation Page

1. Report No.	2. Government Accession No.	3. Recipient's Catalog No.
DOT/FAA/PM-83/33	AD-A141552	

4. Title and Subtitle	5. Report Date
Investigation of the Detectability and Lifetime of Gust Fronts and Other Weather Hazards to Aviation	October 1983
	6. Performing Organization Code
	8. Performing Organization Report No.
7. Author(s)	
Dusan S. Zrnic' and Jean T. Lee	
9. Performing Organization Name and Address	10. Work Unit No. (TRAIS)
U.S. Dept. of Commerce National Oceanic and Atmospheric Administration National Severe Storms Laboratory 1313 Halley Circle, Norman, OK 73069	156-410-01W
	11. Contract or Grant No.
	DTFA01-81-Y-10521
	13. Type of Report and Period Covered
12. Sponsoring Agency Name and Address	Final Report February 1982 to October 1983
U.S. Dept. of Transportation Federal Aviation Administration 800 Independence Ave., S.W. Washington, D.C. 20591	14. Sponsoring Agency Code FAA/APM-310

15. Supplementary Notes

Prepared under Interagency Agreement DTFA 01-81-Y-10521, managed by the Primary Radar Program APM-310

16. Abstract

Low-altitude wind shear associated with diverging outflows has been related to several aircraft accidents. We examine several gust fronts using Doppler radar data and measurements from surface stations and tall tower. We present radar-derived parameters such as reflectivity, height, maximum shear, peak velocity, distance of the front from the producing storm and the nearest 30 dBZ contour for several gust fronts within 60 km of the radar during 1980 to 1982. For all orientations of the front, even along the radial direction, the frontal discontinuity was evident in both mean velocity and spectrum width fields. Thus, while detection is practical with a single Doppler radar, accurate estimation of shear magnitudes is more difficult when the frontal discontinuity is aligned along the radial. Several downdrafts of different sizes are present simultaneously behind some of the fronts and the maximum measured shear of radial velocities produced by one downdraft was $2 \cdot 10^{-2} s^{-1}$. A more typical value of $10^{-2} s^{-1}$ was observed at several locations. Maximum azimuthal shear of $4.7 \cdot 10^{-2} s^{-1}$ occurred at the wave crest.

17. Key Words	18. Distribution Statement
Doppler Radar Gust Front	Document is available to the US public through the National Technical Service, Springfield, VA 22151

19. Security Classif. (of this report)	20. Security Classif. (of this page)	21. No. of Pages	22. Price
Unclassified	Unclassified	58	

Form DOT F 1700.7 (8-72) Reproduction of completed page authorized

METRIC CONVERSION FACTORS

Approximate Conversions to Metric Measures

Symbol	When You Know	Multiply by	To Find	Symbol
	LENGTH			
in	inches	*2.5	centimeters	cm
ft	feet	30	centimeters	cm
yd	yards	0.9	meters	m
mi	miles	1.6	kilometers	km
	AREA			
in^2	square inches	6.5	square centimeters	cm^2
ft^2	square feet	0.09	square meters	m^2
yd^2	square yards	0.8	square meters	m^2
mi^2	square miles	2.6	square kilometers	km^2
	acres	0.4	hectares	ha
	MASS (weight)			
oz	ounces	28	grams	g
lb	pounds	0.45	kilograms	kg
	short tons (2000 lb)	0.9	tonnes	t
	VOLUME			
tsp	teaspoons	5	milliliters	ml
Tbsp	tablespoons	15	milliliters	ml
fl oz	fluid ounces	30	milliliters	ml
c	cups	0.24	liters	l
pt	pints	0.47	liters	l
qt	quarts	0.95	liters	l
gal	gallons	3.8	liters	l
ft^3	cubic feet	0.03	cubic meters	m^3
yd^3	cubic yards	0.76	cubic meters	m^3
	TEMPERATURE (exact)			
°F	Fahrenheit temperature	5/9 (after subtracting 32)	Celsius temperature	°C

*1 in = 2.54 (exactly). For other exact conversions and more detailed tables, see NBS Misc. Publ. 286, Units of Weights and Measures, Price $2.25, SD Catalog No. C13.10:286.

Approximate Conversions from Metric Measures

Symbol	When You Know	Multiply by	To Find	Symbol
	LENGTH			
mm	millimeters	0.04	inches	in
cm	centimeters	0.4	inches	in
m	meters	3.3	feet	ft
m	meters	1.1	yards	yd
km	kilometers	0.6	miles	mi
	AREA			
cm^2	square centimeters	0.16	square inches	in^2
m^2	square meters	1.2	square yards	yd^2
km^2	square kilometers	0.4	square miles	mi^2
ha	hectares (10,000 m^2)	2.5	acres	
	MASS (weight)			
g	grams	0.035	ounces	oz
kg	kilograms	2.2	pounds	lb
t	tonnes (1000 kg)	1.1	short tons	
	VOLUME			
ml	milliliters	0.03	fluid ounces	fl oz
l	liters	2.1	pints	pt
l	liters	1.06	quarts	qt
l	liters	0.26	gallons	gal
m^3	cubic meters	35	cubic feet	ft^3
m^3	cubic meters	1.3	cubic yards	yd^3
	TEMPERATURE (exact)			
°C	Celsius temperature	9/5 (then add 32)	Fahrenheit temperature	°F

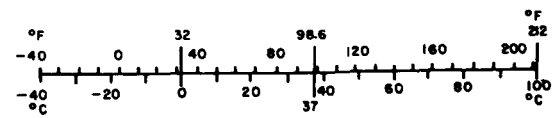

PREFACE

We thank our colleagues of the National Severe Storms Laboratory for support and the fine data sets on which this study was based. Mr. David Lewis helped in data reduction and the tabulations. Dr. R.J. Doviak reviewed this manuscript and gave useful advice during the data analysis phase. Michelle Foster and Joy Walton typed the manuscript, Joan Kimpel performed the artwork, and Robert Goldsmith was the photographer.

TABLE OF CONTENTS

LIST OF FIGURES

LIST OF TABLES

INVESTIGATION OF THE DETECTABILITY AND LIFETIME OF GUST FRONTS AND OTHER WEATHER HAZARDS TO AVIATION

Dusan S. Zrnic' and Jean T. Lee

1. Introduction

The thunderstorm presents one of the greatest obstacles to safe aircraft operation. Thunderstorm power is manifested in wind, turbulence, rain, lightning and hail. One of the most severe events in the thunderstorm is the evaporatively cooled downdraft that, upon reaching the ground, spreads horizontally forming a diverging outflow under the downdraft and a gust fr at the leading edge (Sasaki and Baxter, 1982). The warm, moist, boundary layer air, usually flowing from the south or southeast in the central U.S , is lifted as it flows over the top of this pool of cooled denser air and forms a conspicuous arcus cloud that appears near the front (Figure 1a). ...e front is marked by shifts (shear) in the wind, both in the vertical (Figure 1b) and horizontal directions (Figure 1c). A gust front can propagate in clear air many tens of kilometers away from the thunderstorm that caused it and yet harbor shear forces that can be destructive to aircraft, especially when a flight crew is unaware of its presence. The wind behind the front is usually strong and turbulent, and in the vicinity of the downdraft strongly divergent. The vertical velocities of downdrafts cannot be measured with a Doppler radar whose beam is horizontally directed, but the diverging flow beneath the downdraft produces a telltale signature in the Doppler velocity field. The leading edge of the diverging air often generates a thin zone of enhanced reflectivity. This reflectivity may be so weak ($\leq$10 dBZ) that some radars fail to detect it. However, moderately sensitive Doppler weather radars can sense reflectivities as low as -10 dBZ at range $\leq$60 km.

Weak reflectivity is not the only problem that impedes measurement of wind shear. Storm outflows are relatively shallow (about 500-900 m near the leading edge) and, even at a 0° elevation angle, may fall below the beam at far ranges. Closer in, the ground clutter echoes may overwhelm the signals from the outflow. Furthermore, terrain and buildings can block the antenna beam near the ground, preventing observations at low elevation angles, and second or higher order trip echoes may obscure observation (Doviak and Zrnic',

Figure 1a. A gust front with associated arcus cloud. The bright region is cool, precipitation-free air that has descended to the ground and is spreading out of the picture. The overriding moist inflow is condensing above the outflow, creating the arcus cloud. (Courtesy H. Bluestein, University of Oklahoma)

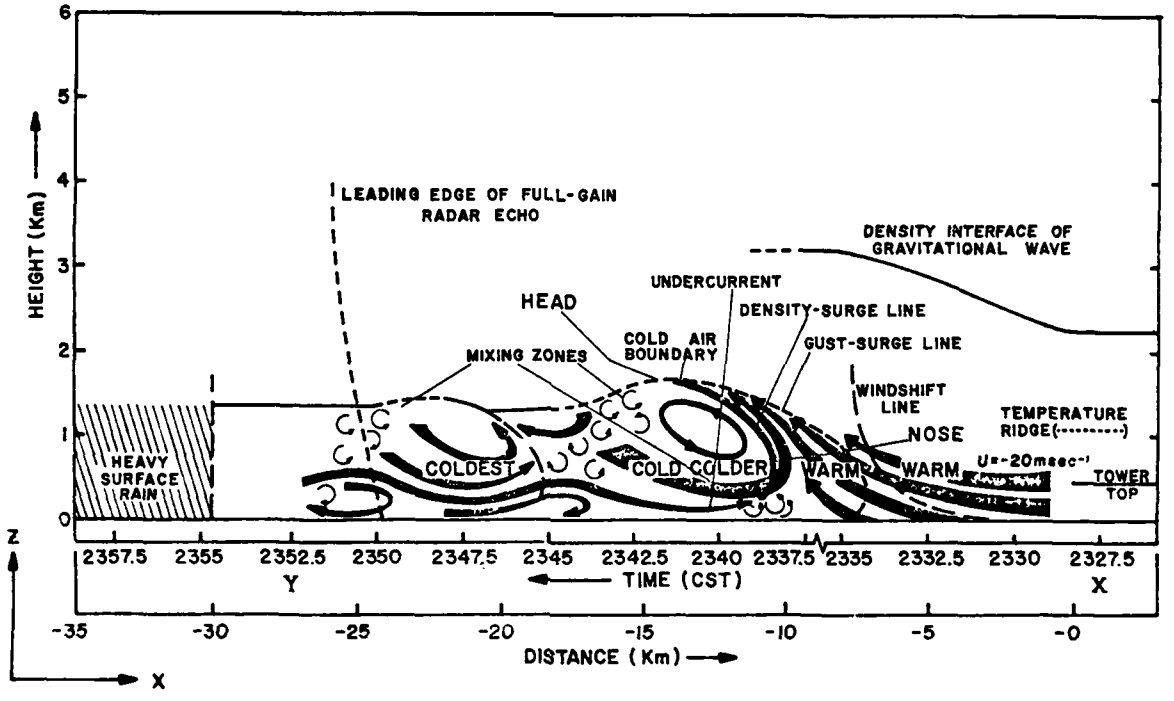

Figure 1b. A composite schematic model combining the features of the analyzed and deduced structure of the windshifts and gust front leading the squall line of May 31, 1969. (After J. Charba, 1974)

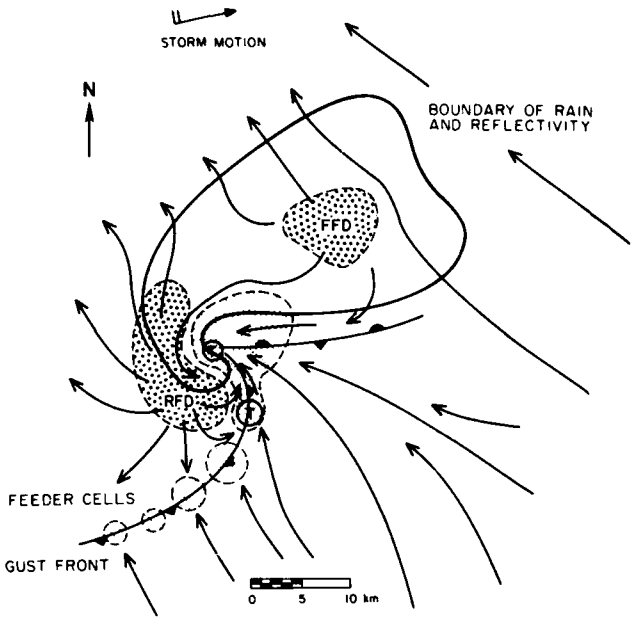

Figure 1c. A schematic of a storm at low levels, with environmental winds, gust front, and a boundary of rain and higher reflectivity. RFD and FFD are rear and forward flank downdrafts. (From R. Davies-Jones, 1982)

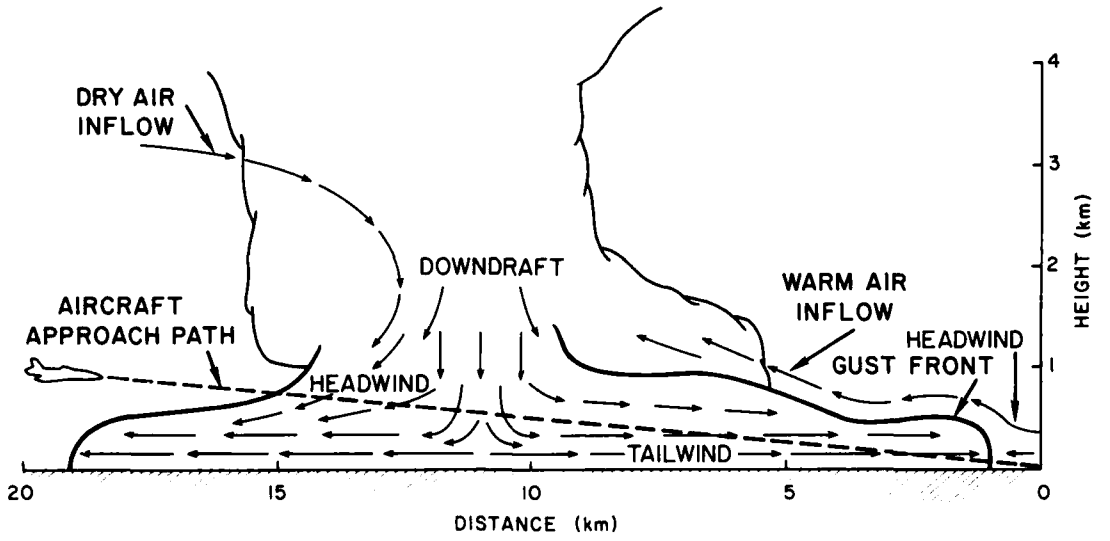

Figure 1d. Schematic of a thunderstorm downdraft and associated gust front on the approach path to an airport. Note the sudden change in the horizontal wind component at the distance of about 11 km. In particular cases and at particular stages in the life of a storm, the horizontal scale of the disturbance may be substantially smaller or larger.

1984). Therefore, detection and tracking of gusts near airports impose a very stringent requirement on siting of the radar (Mahapatra et al., 1983). In order to assess siting alternatives (i.e., most desirable distance from the center of runways), we examine in detail several storm outflows that were recorded by the Norman Doppler radar. In addition to the strong shear at the gust front we have also other dangers to aircraft such as (1) strong turbulence produced by shears at the interface between the outflow and inflow, (2) a large decrease in headwind component (Figure 1d) in the transition zone where the downdraft is converted to strong surface divergence (Lee et al., 1978), and (3) vertically oriented vortices that are well organized and intense.

2. Gust Front Characteristics

Before presenting case studies, we briefly discuss the important parameters that are measurable with a radar. Peak reflectivity factor is read from a PPI display with the cursor if it persists over an area of several km^2. Most fronts had peak reflectivities from 7 to 11 dBZ, and none of the examined ones had less than 2 dBZ. Color categories on our display allow easy readings of -1 dBZ, 2 dBZ, 7 dBZ and up. Therefore, we have tabulated the width of a 2 dBZ contour. The gust's peak radial speed v_{rm} is the maximum measured radial velocity immediately behind the gust front (Figure 2). Fronts are well defined on the color displays by abrupt changes in radial velocity and a line of large spectrum width σ_v. Maximum shear across the front is obtained by (1) assuming that gust air moves perpendicular to the front, (2) assuming that velocities are uniform along the front, and (3) calculating the speed from

$$v_m = v_{rm}/\cos\alpha \qquad (1)$$

where α is the angle between the perpendicular to the tangent and the radial. The environmental wind v_e at ground level is obtained by averaging surface wind measurements ahead of the front. Then the magnitude of horizontal shear is estimated as

$$k_h = \frac{|\vec{v}_m - \vec{v}_e|}{d_f} \qquad (2)$$

where d_f is the distance between the location of the peak gust and the front.

Values of gust front parameters from seven cases are tabulated in the appendix. These were estimated from the time the gust was first recorded until the end of data collection. Except in one case, all analysis is done with the help of a playback display. The cursor in this display is used to read off parameters such as height, range, azimuth, velocity, and reflectivity. The uncertainty in reflectivity due to quantization is about 3 dB at low values of interest. In some cases 10 dBZ was added to all reflectivities on a display in order to bring weak ones above the threshold which is fixed at 9 dBZ and cannot be easily changed. Velocity quantization was between 2 and 4 $m \cdot s^{-1}$. Resolution of measured distances is dictated by the beamwidth and the spacing between consecutive gates that are displayed. Typically these are about 300 m in range and 1° in azimuth. The height is to beam center above ground and the sampling at lowest elevations was spaced by 0.4° so that the resolution is about a beamwidth. Because a 30 dBZ contour can be considered to be the edge of significant precipitation (rain rate R of about 3 mm/h when a relationship $Z=200R^{1.6}$ is valid), we have tabulated the distance from the nearest 30 dBZ contour to the front.

The data from the Appendix are summarized in Table 1. The values bracket the range from the minimum to the maximum for each case. Where there is only one value, both the maximum and minimum were within one quantization interval. Maximum shear (radar) signifies measurements that were obtained from the radar and surface stations via (2). Maximum shear (surface station) was obtained from each surface station during the passage of the front. The propagation speed of the front was estimated from the radar data in order to transform time to space.

To help the reader relate the positions of fronts to the location of surface stations, we present on Figure 3 the map around Norman with the surface stations. Graphs of wind speed and direction were plotted for each surface station for the times of the frontal passages. A typical example (Figure 4) consists of one minute average wind speeds and maximum wind speeds over one minute intervals. The maximum wind shear calculated from average velocities (between times 0049 and 0052 CST) is lower than the one obtained from maximum velocities. This was consistently the case at all surface stations (see Tables 2a and 2b) so we opted to summarize in Table 1 the higher values.

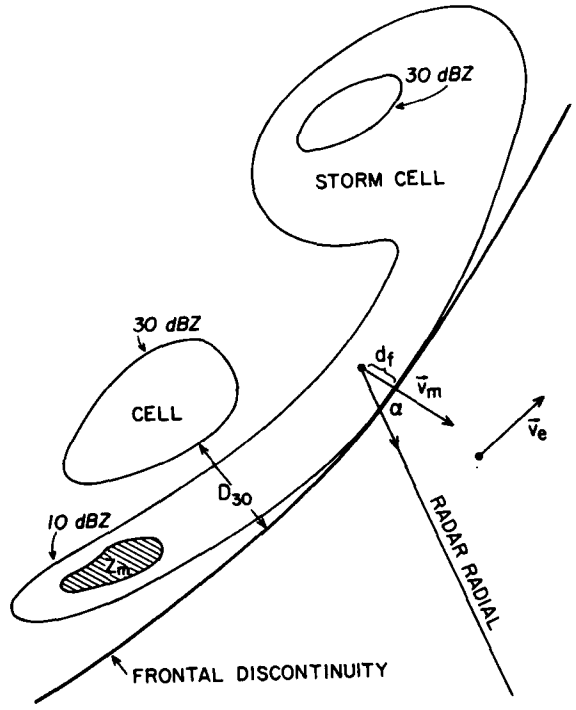

Figure 2. Schematic of a gust front.

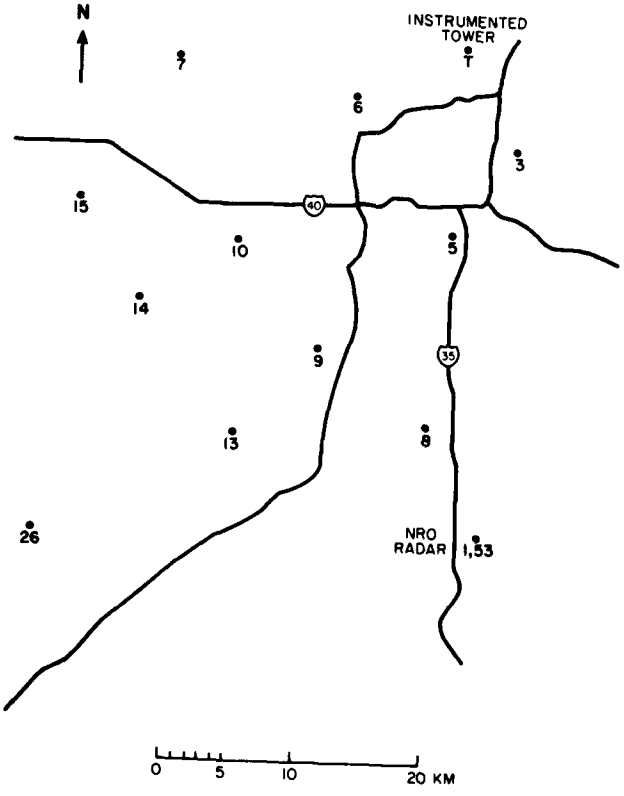

Figure 3. Locations of the surface stations and the Norman radar.

TABLE 1

SUMMARY OF GUST FRONT CHARACTERISTICS

	5-17-80	5-29-80	6-16-80	4-10-81	4-13-81	4-30-81	5-8-81
Height (km)	0.5-2.9	0.1-1.3	0.1-0.6	0.2-1.1	0.4-1.8	0.2-1.9	0.1-2.8
Peak Refl. (dBZ)	11	45*	11	7-11	2-11	11-21*	11
Width of Refl. >2 dBZ (km)	2-13	10-20	2-5	2.5-12	1-10	1-12	4-15
Range from nearest 30 dBZ to front (km)	4-30	0	16-25	6-24	9-25	2-25	20-65
Length (km)	30-80	40-70	30	60-92	15-80	12-55	50-95
Peak Gust v_{mr} Speed (magnitudes) ($m \cdot s^{-1}$)	18-32	18-32	16-23	13-28	6-23	7-23	20-31
Max. Shear x 10^3 (radar) (s^{-1})	7-34	5-13	7-40	11-42	3-49	4-129	9-39
Max. Shear x 10^3 (surface station) (s^{-1})	2.1-7.9	1.4-5.6	1.4-4.5	2.9-7	2-6.4	1.3-1.6	2.3-4.5
Propagation speed of the front ($m \cdot s^{-1}$)	15	15	5	20	18	8	18

*These reflectivities were in precipitation.

TABLE 2a

WINDSHEAR DATA (s^{-1})
from
SURFACE STATIONS
(calculated from peak velocities within 1 minute intervals)

Date/ Station	5/17/80	5/29/80	6/16/80	4/10-11/81	4/13/81	4/30/81	5/9/81
1	.0064	.0050	.0031				.0035
3	.0021		.0014		.0036		.0027
5	.0041	.0014			.0020		.0037
6	.0029		.0045		.0064		.0042
7	.0039						.0039
8				.0029			.0039
9				.0039	.0064		.0036
10	.0039			.0048			.0034
13	.0052	.0056		.0047	.0038		.0045
14				.0070			
15	.0053			.0044			
26	.0079	.0054		.0052		.0016	.0036
53	.0075			.0034	.0036		.0029
54					.0022	.0013	.0023

TABLE 2b

WINDSHEAR DATA (s^{-1})
from
SURFACE STATIONS
(calculated from one minute averages of velocities)

Date/ Station	5/17/80	5/29/80	6/16/80	4/10-11/81	4/13/81	4/30/81	5/9/81
1	.0048	.0035	.0014				.0026
3	.0016		.0011		.0023		.0022
5	.0028	.0010			.0014		.0027
6	.0024		.0022		.0035		.0029
7	.0028						.0032
8				.0022			.0030
9				.0024	.0028		.0026
10	.0031			.0031			.0025
13	.0030	.0049		.0033	.0023		.0031
14				.0038			
15	.0031			.0034			
26	.0060	.0037		.0036		.0008	.0025
53	.0053			.0025	.0025		.0024
54					.0012	.0008	.0019

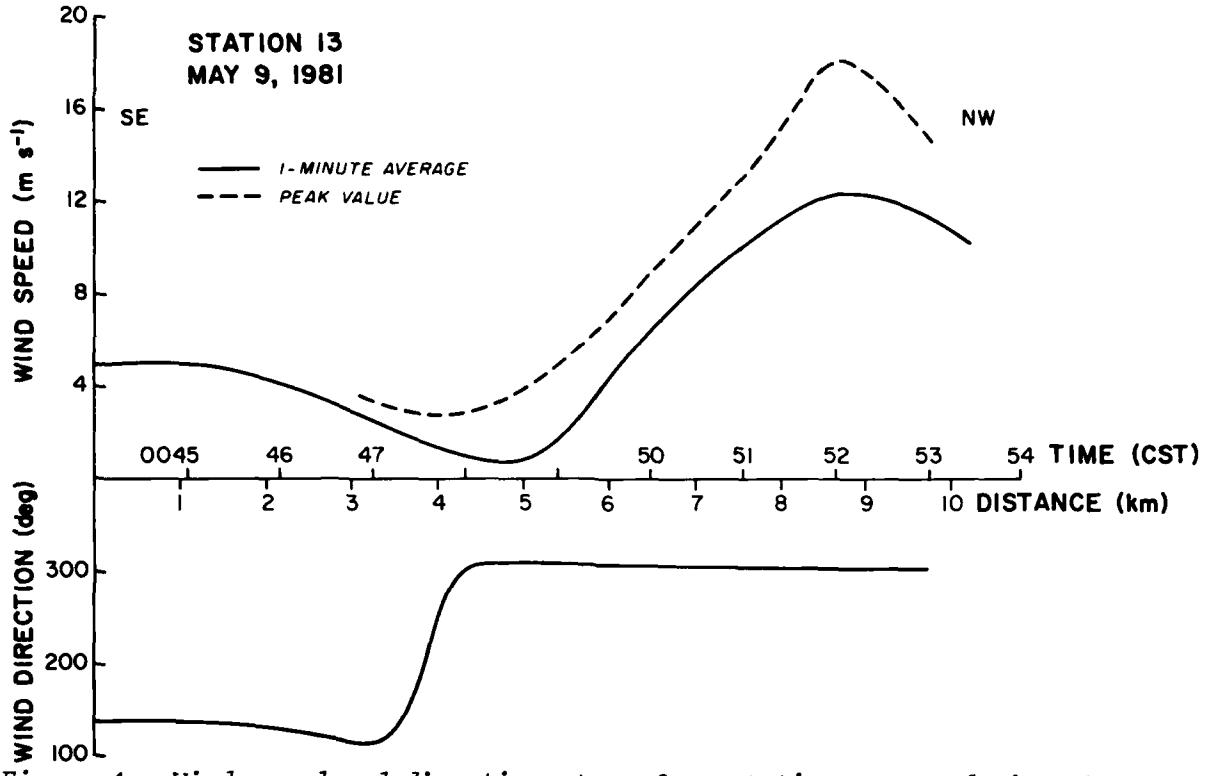

Figure 4. Wind speed and direction at surface station No. 13 during the passage of the May 9, 1981, gust front.

We see (Table 1) that the minimum peak reflectivity is 2 dBZ and the width of such a contour is at least 1 km. Range to the nearest 30 dBZ contour is quite variable but could be as high as 65 km. Thus, avoiding regions of significant reflectivity does not guarantee trouble-free flights. The lengths of these fronts are also variable, but the maximum speeds v_m have a good consistency. The shears calculated using radar and surface observations for v_e are consistently and considerably higher than the ones calculated from surface observations alone. Higher values are expected because radar-measured velocities are representative of values hundreds of meters above ground where speeds are two to three times higher than near the ground. For instance on May 17, 1980, the radar measured velocity at 500 m above ground was 27 $m \cdot s^{-1}$ whereas the surface station No. 13 measured 9 $m \cdot s^{-1}$. This gives a vertical shear of horizontal wind of 0.036 s^{-1} which accounts for the discrepancy in Table 1.

3. Case Examples

In the following we discuss, in chronological order, eight example cases and show color photographs and the display of the three spectral moments. Corresponding tables in the appendix are noted for seven dates.

3.1 5/17/80 (Table A.1)

This front was produced by a strong squall line with reflectivities of 60 dBZ (Figure 5a). Peak radial velocities of 29 $m \cdot s^{-1}$ were measured--red patch in the midst of green velocities on Figure 5b. The zero velocity category clearly delineates the front's position. Note that the spectrum width field (Figure 5c) depicts the frontal discontinuity even in a region where the edge of the front is aligned along the radial (cursor on Figure 5b and 5c). Thus, even in cases when the front moves perpendicular to the radial, spectrum width data may offer a good signature of the gust front location. With the gust front velocity removed, several signatures of divergent flow become apparent (Figures 5d and 5e). Sizes of these range from 2 to 10 km and suggest presence of downdrafts. In this one and most other gusts associated with intense, wet Oklahoma systems, the presence of downdrafts is also accompanied by very turbulent eddies, which are evident on the spectrum width display (Figure 5c). The strong variations in velocity behind the front (Figure 5b) are produced by the constantly evolving and interacting cells that generate short-lived up/down drafts. Therefore, it would not be prudent to attempt landing or takeoff of aircraft behind fronts of this type. Note that PanAm Flight 759 at New Orleans International Airport took off during the passage of a gust front or shortly thereafter (Fujita 1983). Maximum radial shear of $2 \cdot 10^{-2} s^{-1}$ was produced by a small downdraft, and it was measured with the beam center at 800 m above ground. Maximum azimuthal shear of $4.7 \cdot 10^{-2} s^{-1}$ was detected near the wave crest. Presence of a vortex can produce a large decrease in headwind component if the aircraft path is tangent to the circle of maximum wind (Figure 6). Thus, for this example the encountered shear could be about $2.35 \cdot 10^{-2} s^{-1}$. At several locations behind the front we have measured radial shears of $1 \cdot 10^{-2} s^{-1}$. The maximum difference of outflow velocities produced by these downdrafts depends little on the signature diameter and therefore the maximum measured shear is associated with smallest sizes!

(a)

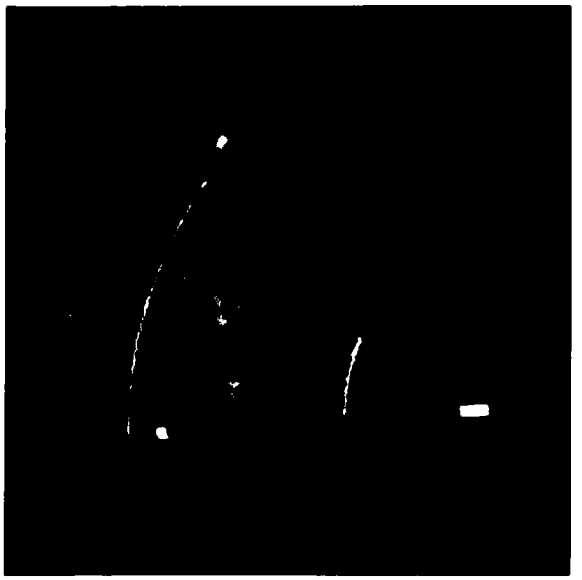

(b)

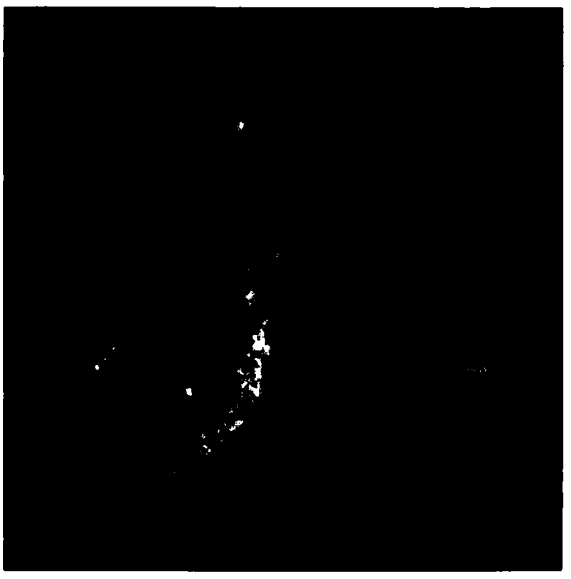

(c)

Figure 5. Gust front of May 17, 1980. a) Reflectivity display. Color categories in dBZ are indicated. Range rings are 20 km apart and height of cursor is 700 m; elevation is 0.9°.

b) Mean velocity display. Negative velocities are towards the radar.

c) Doppler spectrum width. Displayed values are for data which have at least a 20 dB signal-to-noise ratio.

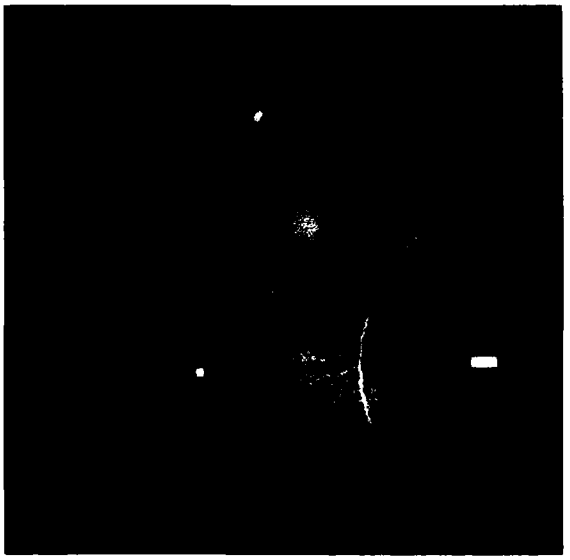

(d)

Figure 5. Gust front of May 17, 1980. d) Same as (b) but mean speed of 15 $m \cdot s^{-1}$ from 260° has been removed.

e)Same as (d) but at the next elevation of 1.3°.

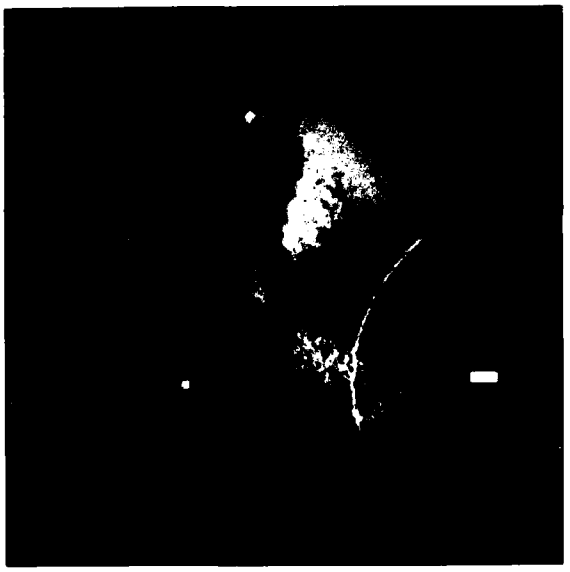

(e)

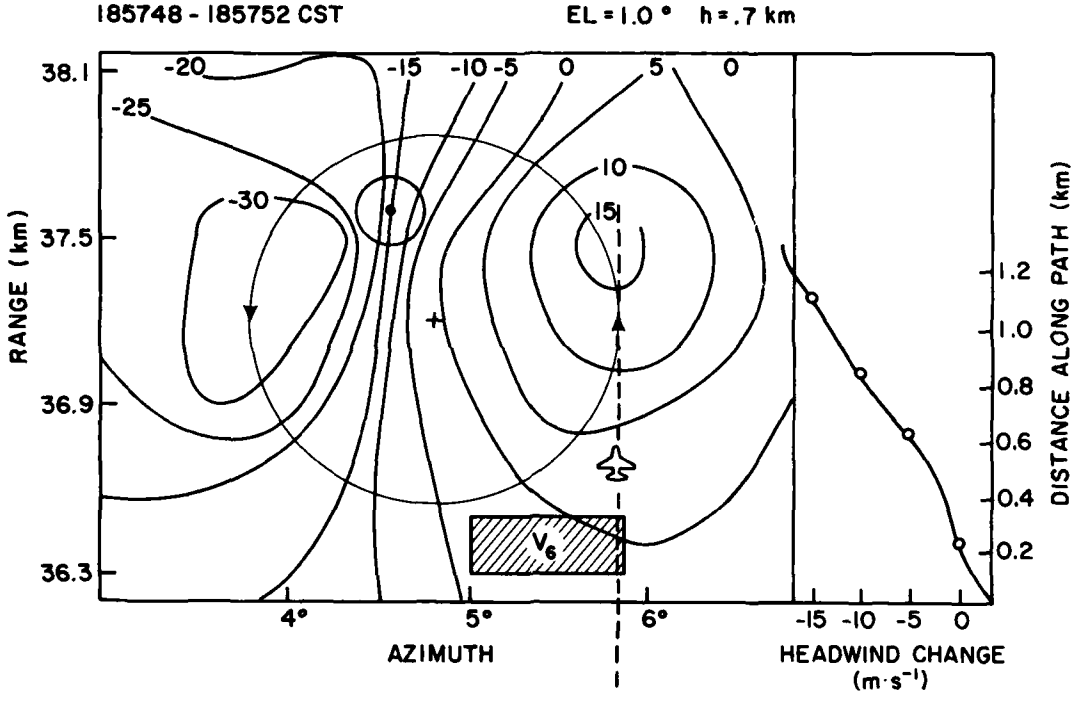

Figure 6. Doppler radial velocities of a mesocyclone at 0.7 km above ground. The cross indicates cyclone and the small circle with a dot is the position of a tornado. Size of the radar resolution volume V_6 is indicated. A hypothetical aircraft path is tangent to the circle of maximum wind and the corresponding headwind change is plotted on the right side of the graph.

3.2 5/29/80 (Table A.2)

The frontal discontinuity in the data collected is part of a squall that passed over the radar. Peak reflectivities of the storm are at most 50 dBZ, yet winds are as high as 32 $m \cdot s^{-1}$ (Figures 7a and 7b). Note that the spectrum width field indicates well the frontal boundary (Figure 7c). Both the mean velocity and spectrum width depict nicely the discontinuity even when it is aligned with the radial (30 to 40 km at 150°). Note that the frontal discontinuity exhibits a "line echo wave pattern", which Nolen (1959) defined as a sinusoidal mesoscale wave pattern in which a line of echoes has been subjected to an acceleration along one portion and/or deceleration along the portion of the line immediately adjacent. The velocity field suggests a presence of a mesolow pressure in which acceleration of the environmental wind near the gust and inflow into the storm are in accordance with the conceptual model of Figure 1c. Analysis by Lee et al. (1978) of similar data from two Doppler radars has confirmed a circular eddy pattern. The cyclonic couplet (30 to 40 km at 180°, Figure 7b) extends only to 2.8 km in height, and the flow above is that of the environment. The largest spectrum widths (Fig. 7b) are in the couplet's center, suggesting that there shear and turbulence are most intense.

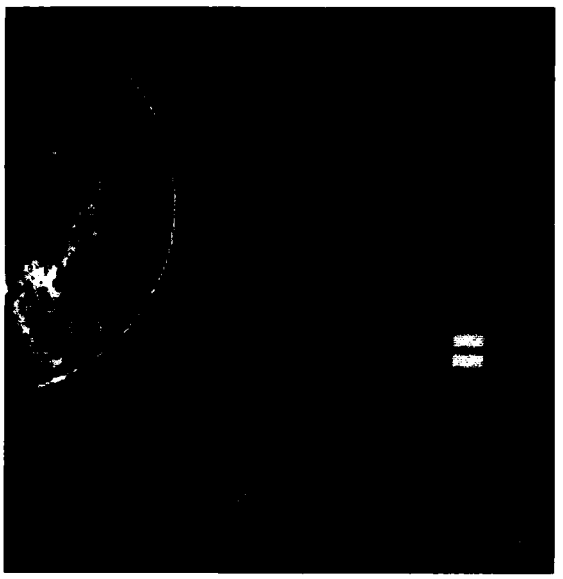

(a)

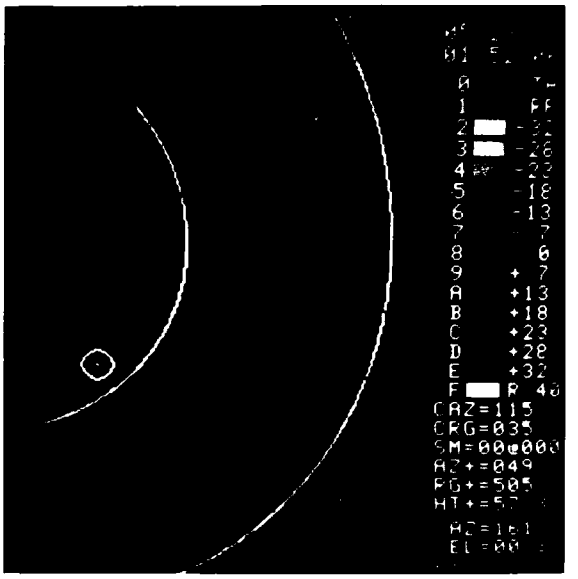

(b)

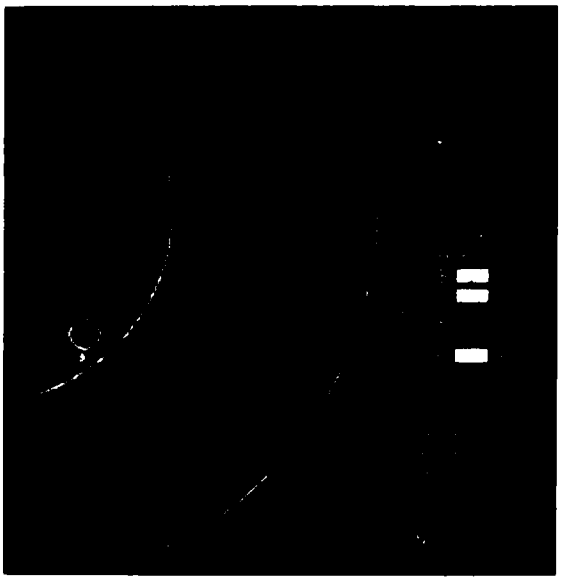

(c)

Figure 7. Squall line of May 29, 1980.
a) Reflectivity.

b) Velocity.

c) Spectrum width at an elevation of 0.8°.

Range marks are 40 km apart.

3.3 6/16/80 (Table A.3)

A gust front at about 30 km from the generating storm was recorded on this day. Because of the ground clutter it is barely visible on the reflectivity display (Figure 8a) even though 10 dBZ was added to all reflectivities to bring them above the threshold. Peak reflectivity is about 11 dBZ, and the width of a 2 dBZ contour is only 2 to 5 km. Because of the relatively low height and reflectivity, this type of front will impose stringent demands on the airport surveillance radar. Both the velocity discontinuity (Figure 8b) and enhanced spectrum width (Figure 8c) are present (near the cursor) at about 30 km from the radar. But without the ground clutter canceler, the information would be lost at ranges closer than 20 km for the Norman site.

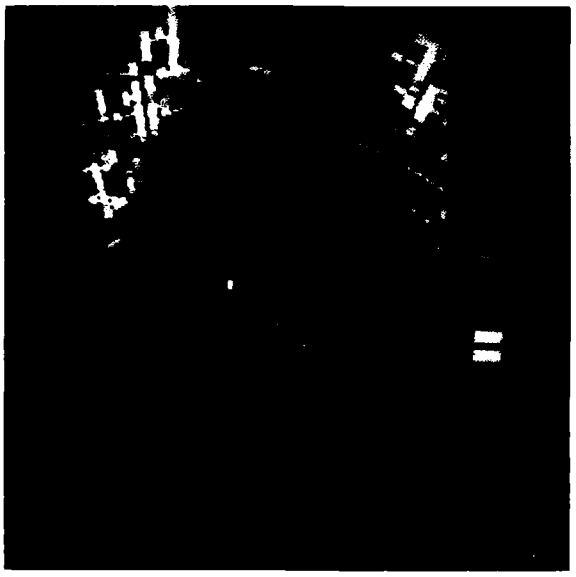

(a)

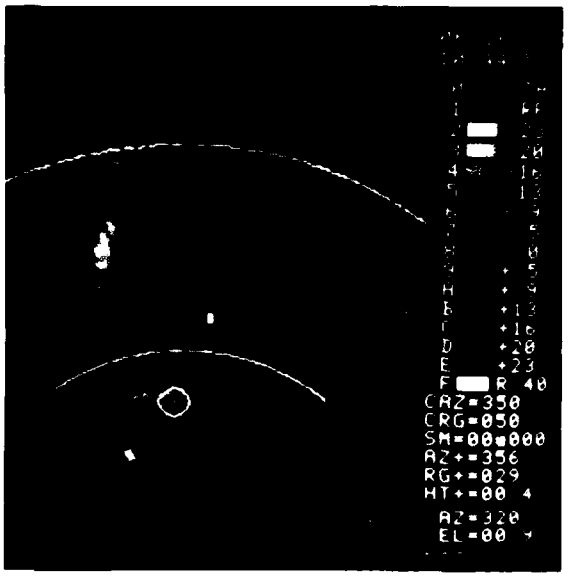

(b)

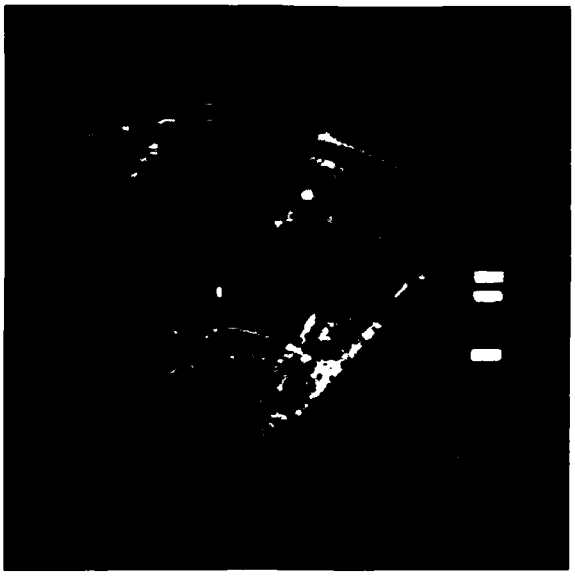

(c)

Figure 8. Gust front from June 16, 1980. a) Reflectivity--the scale is 10 dBZ higher than the actual values.

b) Velocity.

c) Spectrum width.

Range marks are 40 km apart.

3.4 4/10/81 (Table A.4)

An instructive example of a squall with a frontal discontinuity along a radial was collected on April 10, 1981 (Figures 9a, b, c). Again the velocity field depicts precisely its location. Note the acceleration of the environmental wind ahead of the front (Figure 9b) and the associated increased spectrum width (Figure 9c). Very similar general features can be seen on the display 40 minutes later in Figures 9d, e, f, but the smaller structures have evolved considerably. Thus, volume update rates of 5 minutes should be sufficent to track gusts like these, which harbor short-lived intense phenomena.

(a)

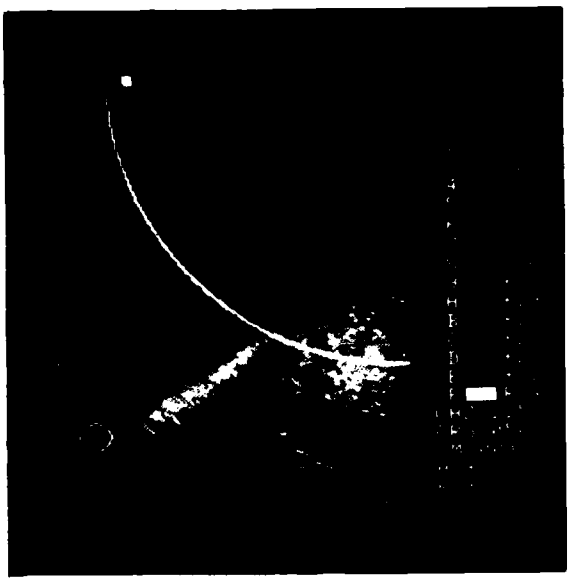

(b)

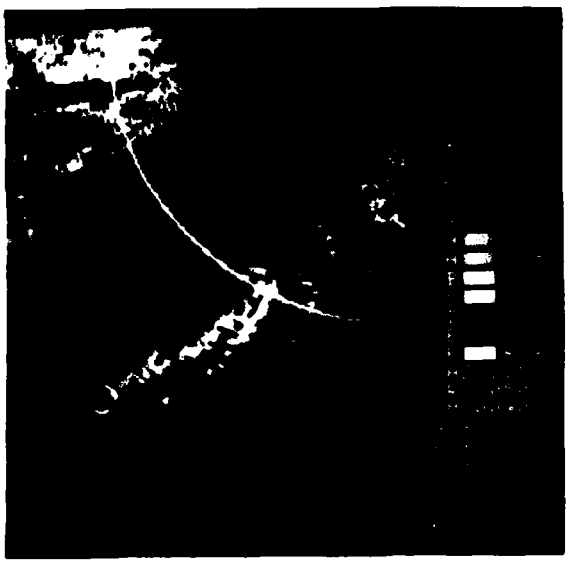

(c)

Figure 9. April 10, 1981.
a) Reflectivity--the scale is 10 dBZ higher than the actual values.

b) Velocity.

c) Spectrum width--signal-to-noise threshold on this display is low (0 dB) and that is the reason why widths on the edge of echoes are high.

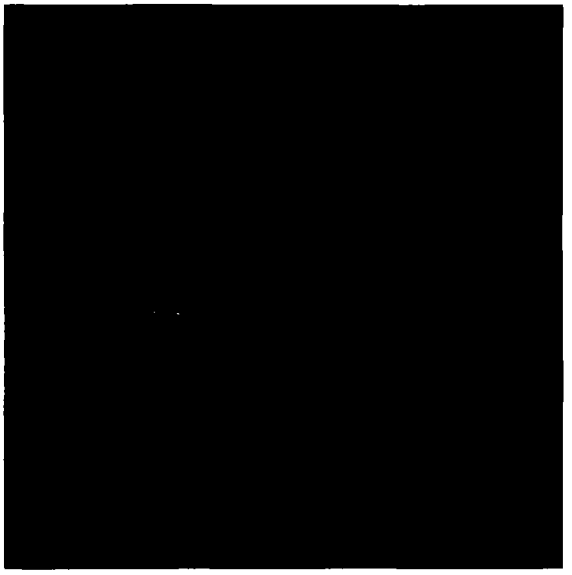

(d)

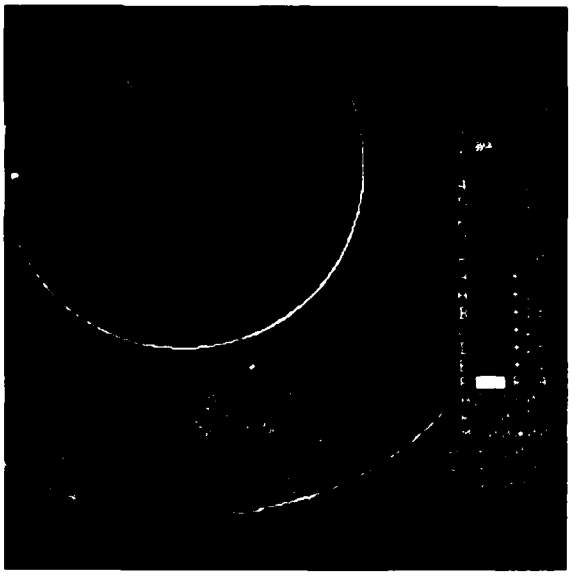

(e)

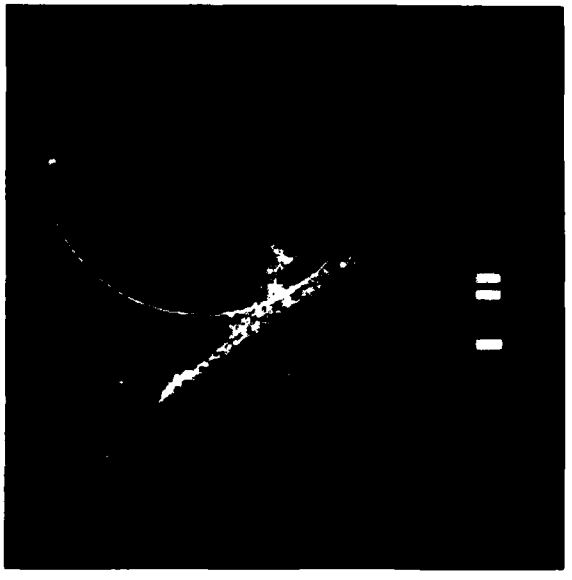

(f)

Figure 9. April 10, 1981.
d) Reflectivity at a later time (10 dBZ higher than actual.

e) Velocity.

f) Spectrum width--the signal-to-noise threshold is 8 dB.

Range marks are 40 km apart.

3.5 4/13/81 (Table A.5)

A very intense front developed in a squall that passed by some surface sites and over Cimarron on this day. At 2056 CST a gust front was observed at 80 km from the radar (Figure 10a, b). It appears that the outflow air is quite distant from the parent storm similar to the case reported by Lee and Doviak (1981); i.e., there is a thin line of air flowing away from the storm. We do not have measurement near the ground, but from the large size of the weak reflectivity behind the front and its shape we deduce that the front's southwestern edge is attached to the storm. Half an hour later the storms moved closer and produced an intense outflow (Figure 10c, d, e, f). The shape and intensity are extremely similar to the May 17 case of 1980 (Figure 5). Note the richness of velocity structure on Figure 10d suggestive of turbulent eddies, which is also present on the spectrum width display (Figure 10f). In its northern part the front is shallow, and above it the flow is from the south as evidenced on Figure 10e (south of the cursor). Note that although the frontal boundary is not apparent at this height on the velocity display between the cursor and the 40 km range mark (Figure 10e), it is clearly visible in the spectrum width field (Figure 10f).

(a)

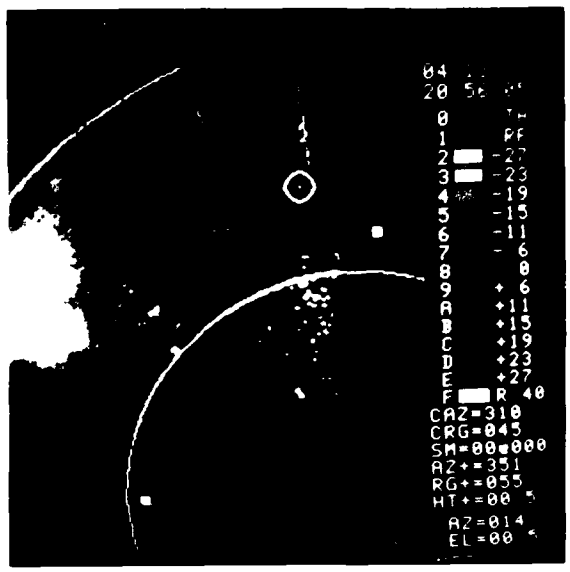

(b)

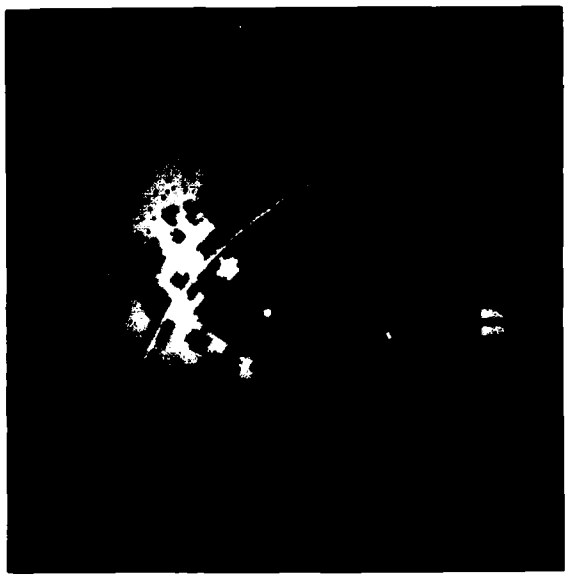

(c)

Figure 10. April 13, 1981.
a) Reflectivity with a scale indicating values higher by 10 dBZ.

b) Velocity--range marks are 40 km apart.

c) Reflectivity at a later time--scale indicates actual values, and range marks are 20 km apart.

(d)

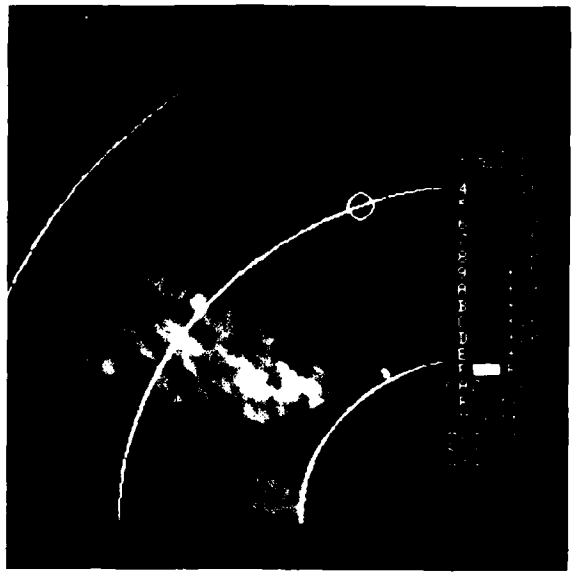

(e)

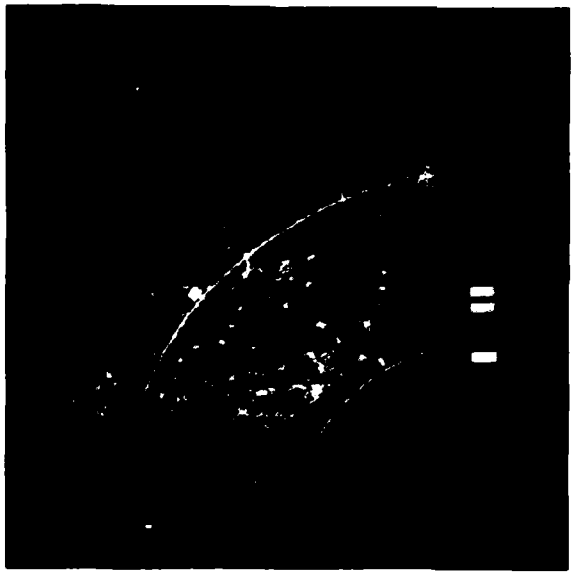

(f)

Figure 10. April 13, 1981.
d) Velocity field.

e) Velocity at an elevation of 2.8°.

f) Spectrum width at 2.8° elevation.

3.6 4/30/81 (Table A.6)

In this instance the gust front was more than 80 km away and could still be seen at the lowest elevation (0.2° on Figure 11a, b).

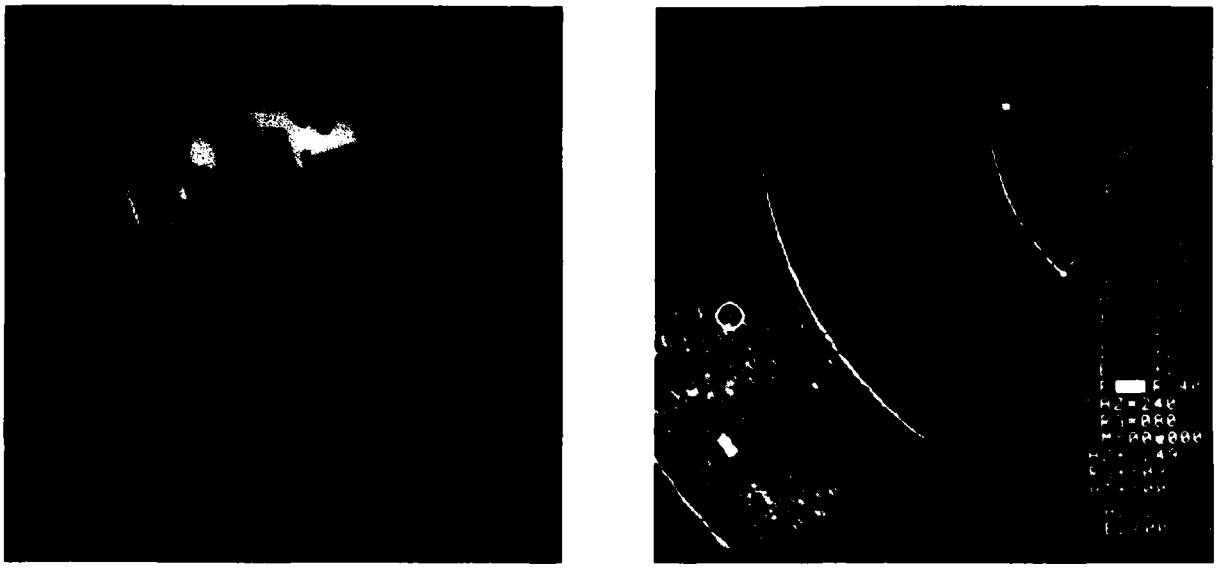

(a) (b)

Figure 11. April 30, 1981.
a) Reflectivity with a 10 dBZ value added.

b) Velocity--range marks are 40 km apart.

3.7 5/9/81 (Table A.7)

The thin line seen in Figure 12a marks the leading edge of the front and is thought to be generated by debris made airborne by the strong gust winds immediately behind the front. Farther back from the front the flow is often less turbulent, and debris settles out so that reflectivity becomes weak. A vertical cross section of the reflectivity field is shown in Figure 12b. These reflectivities are averages over the azimuth sector 305-310°. There are no unique conclusions concerning the nature of tracers in the gust front that is ahead of precipitation. Wakimoto (1982) suggested that a "precipitation roll" carrying small hydrometeors is deflected upward by the ground and thus seen as a thin line on reflectivity displays. We point out that debris and/or refractive index fluctuations may be significant contributors to the reflectivity ahead of the front. The elongated shape of the 5 dBZ contour in the direction of inflow indicates that the inflow could have carried the debris over the leading edge of the front. However, the contrast between warm and cold air mass is quite strong so that strong gradients of potential refractive index may exist and mixing of these could have enhanced the reflectivity (Doviak and Zrnic', 1983).

Even though the single Doppler radar measures only the radial component of the vector wind, we can, by assuming the gust winds are directed perpendicular to the front, obtain the horizontal and vertical wind components from the continuity equation. Radial velocities averaged over the azimuthal interval 305-310° (between the cursor and square mark on Figure 12a) were used to obtain the vector winds plotted onto the vertical cross section in Figure 12b. This gust front, observed shortly after midnight, was extremely strong with vertical winds in excess of 20 $m \cdot s^{-1}$. The turbulent winds associated with this gust extended to altitudes of at least 3 km, above which weak reflectivity precluded measurements. In this case the strong shear regions were 10 km away from the higher reflectivity regions associated with precipitation.

The frontal boundary in the mean velocity display (Figure 12c) is quite distinct, but it becomes diffuse in the spectrum width display (Figure 12d) because the width is more susceptible to contamination from the ground clutter.

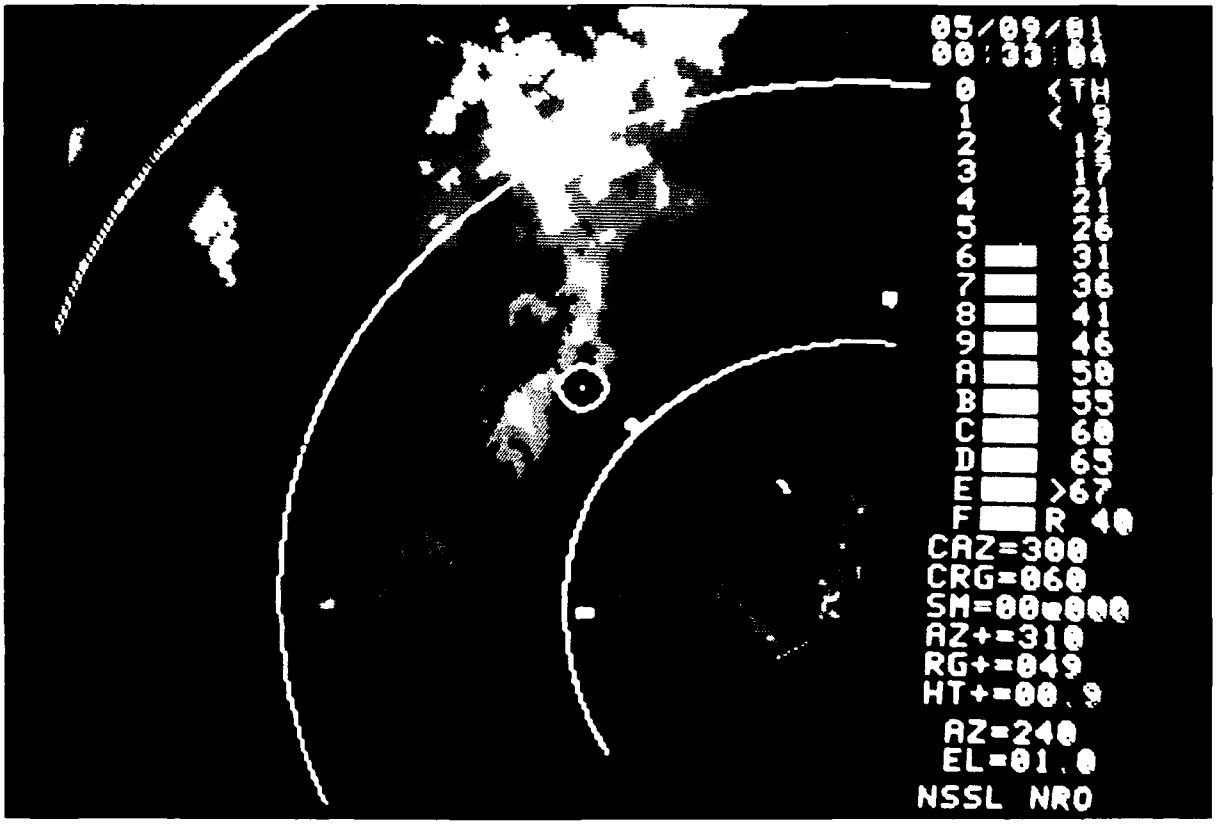

Figure 12a. Reflectivity field of a front that occurred on May 9, 1981. Range marks are 40 km apart.

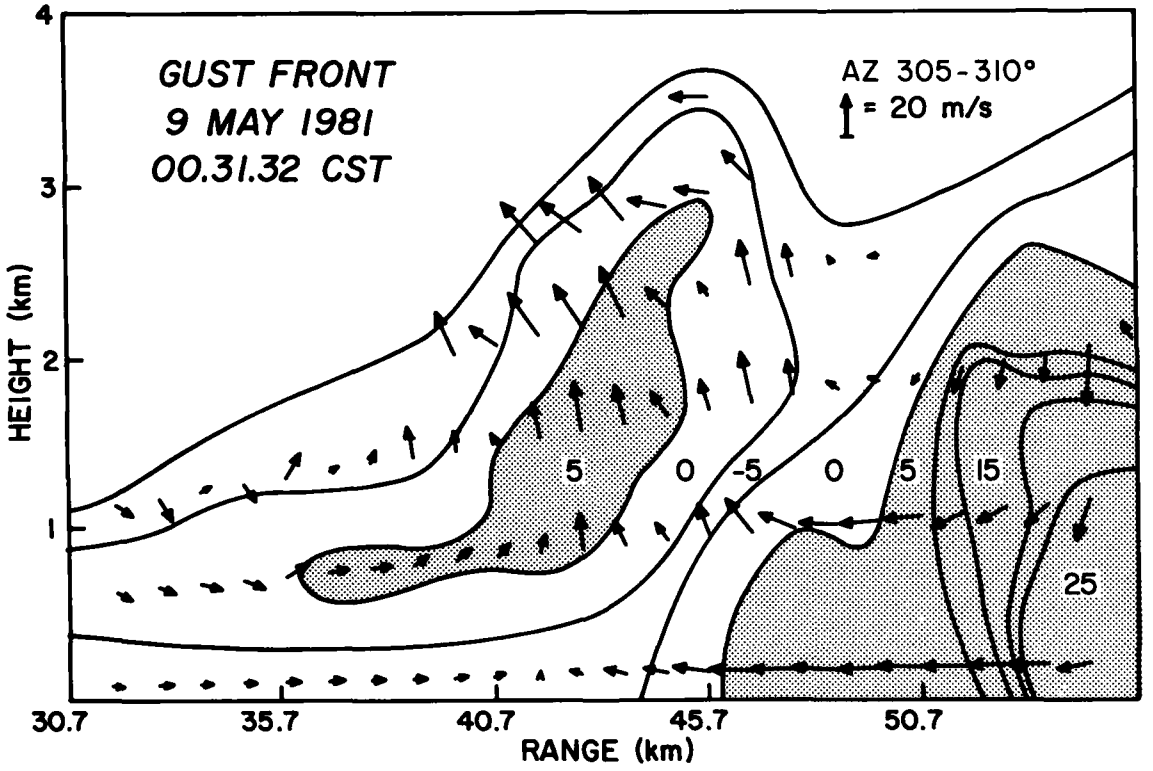

Figure 12b. A vertical cross section of the May 9 gust front. Wind vectors are the horizontal and vertical components in the plane of observation and the 20 $m \cdot s^{-1}$ vector in the upper right corner scales the others. Reflectivity factor, dBZ contours are in steps of 5 dBZ, and the stippled areas start at 5 dBZ. (Analysis by Robin King, Finnish Meteorology Inst., Helsinki, Finland).

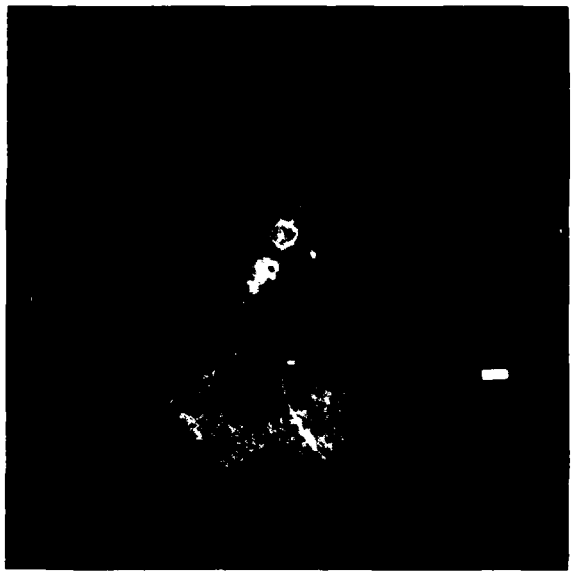

Figure 12c. Velocity field for the May 9, 1981, gust front.

Figure 12d. Spectrum width field.

3.8 5/27/82

This last example consists of a frontal boundary that follows a 30 dBZ reflectivity contour (Figure 13a). The front is seen in the velocity field (Figure 13b) but is most pronounced in the spectrum width data (Figure 13c). Note very large widths (more than 8 $m \cdot s^{-1}$) in echo regions of strong signals (30 dBZ) behind the front. The variability in the velocity and spectrum width fields suggests presence of strong turbulence behind this front.

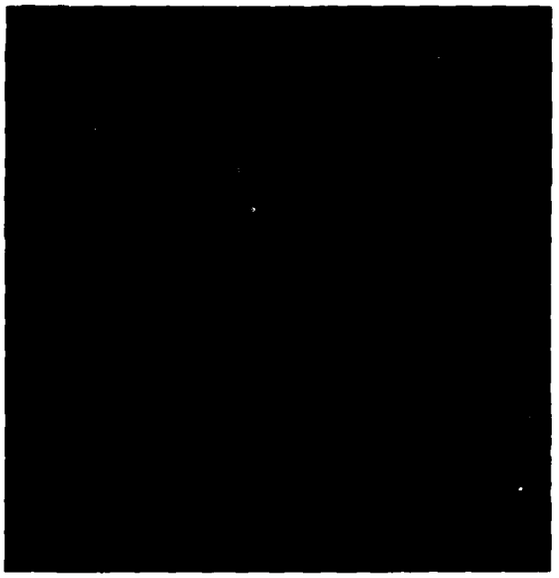

(a)

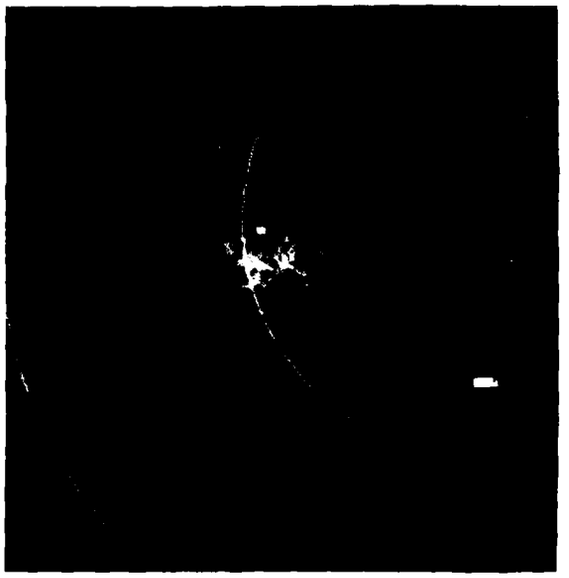

(b)

(c)

Figure 13. May 27, 1982.
a) Reflectivity.

b) Velocity.

c) Spectrum width.

Range rings are 40 km apart.

4. Conclusions

Some characteristics of low-level weather features that may be hazardous in aircraft terminal area have been examined. We considered gust fronts associated with strong squalls in Oklahoma, and downdrafts behind these fronts. We found that peak reflectivity of the gust front (out of precipitation) is between 2 and 11 dBZ.

Half a dozen downdrafts of different sizes seemed to be present simultaneously behind a strong front, and the maximum measured shear of radial velocities was $2 \cdot 10^{-2} s^{-1}$. A more typical value of $10^{-2} s^{-1}$ was observed at several locations. Maximum azimuthal shear of $4.7 \cdot 10^{-2} s^{-1}$ occurred at the wave crest. For all orientations of the front, even along the radial direction, the frontal discontinuity was evident in both mean velocity and spectrum width fields. A mesocyclone-like signature is found and that is where strong azimuthal shear exists. This circulation may produce a large decrease in headwind component of an aircraft. Because of intense turbulence, and changes in headwind tailwind components, we do not recommend that aircraft land or take off in or behind strong gust fronts. It would be a dangerous mistake even to try to meander aircraft through such weather systems.

REFERENCES

Charba, J. 1974: Application of gravity current model to analysis of squall-line gust front. Mon. Weather Rev., 102, 140-156.

Davies-Jones, R.P., 1982: Tornado Dynamics. Thunderstorms: A Social, Scientific, and Technological Documentary, Vol. 2--Thunderstorm Morphology and Dynamics, Editor, Edwin Kessler, U.S. Dept. of Commerce, NOAA, 297-361. (Available fr. the Superintendent of Documents, U.S. Gov. Printing Ofc., Washington, D.C. 20402.)

Doviak, R.J., and D.S. Zrnic', 1984: Doppler Radar and Weather Observations. To be published by Academic Press, New York, NY.

Fujita, T.T., 1983: Microburst wind shear at New Orleans International Airport, Kenner, Louisiana on July 9, 1982. SMRP Research Paper No. 199, Department of Geophysical Sciences, The University of Chicago.

Lee, J.T., J. Stokes, Y. Sasaki, T. Baxter, 1978: Thunderstorm gust fronts - Observations and modeling. FAA Rept. No. FAA-RD-78-145.

Lee, J.T., and R.J. Doviak, 1981: Field program operations - Turbulence and gust front studies. FAA Final Rept. No. DOT/FAA/RD-81/108.

Mahapatra, P.R., D.S. Zrnic', and R.J. Doviak, 1983: Optimum siting of NEXRAD to detect hazardous weather at airports. J. of Aircraft, 20, 363-371.

Nolen, R.H., 1959: A radar pattern associated with tornadoes. Bull. Amer. Meteor. Soc., 40, 277-279.

Sasaki, Y.K., and T.L. Baxter, 1982: The gust front. In Thunderstorms: A Social Scientific and Technological Documentary. Vol. 2, Editor, E. Kessler, U.S. Dept. of Commerce, NOAA, 281-296. (Available from Superintendent of Documents, U.S. Gov. Printing Ofc., Washington, D.C. 20402).

Wakimoto, R.M., 1982: The life cycle of thunderstorm gust fronts as viewed with Doppler radar and rawinsonde data. Monthly Wea. Review, 110, 1060-1082.

APPENDIX

Tables with gust front parameters estimated from the data that were obtained with a single Doppler radar

Data (top to bottom) are from sequential scans.

TABLE A.1

May 17, 1980

Height (km)	Peak Reflectivity (dBZ)	Peak Gust Speed (m/s)	Distance Between Peak Gust Speed and Environmental Wind (km)	Width of Reflectivity Greater Than 2 dBZ (km)	Range of Radar to Peak Gust (km)	Range From Generating Storm to Gust Front (km)	Range From Nearest 30 dBZ to Front (km)	Length (km)	Wind Shear s^{-1}
1.5	11	-18	1	2	142	5	5	30	.024
1.5	11	-28	1	2	143	5	5	30	.034
1.5	11	-28	1.5	3	136	6	6	30	.023
1.5	11	-20	3	5	128	6	6	45	.009
1.3	11	-20	3	5	118	6	6	50	.009
1.2	11	-20	3	4	106	10	10	55	.009
1.9	11	-20	3	4	110	15	15	55	.009
.6	11	-23	3	3	102	18	18	60	.010
.6	11	-23	2	4	96	18	18	65	.014
2.3	11	-23	3	3	95	10	10	55	.010
.5	11	-23	3	4	92	20	20	65	.010
2.1	11	-23	1	3	90	12	12	60	.030
.5	11	-23	2	4	85	20	20	65	.014
2.1	11	-23	2	3	85	12	12	60	.014
.5	11	-23	3	6	74	15	15	65	.001
1.4	11	-23	2.5	5	77	15	15	65	.012
2.6	11	-23	2.5	4	74	15	15	60	.012
.2	11	-23	4	10	59	20	20	70	.007
1.4	11	-23	3	10	59	15	15	70	.010
1.9	11	-23	2.5	5	59	10	10	65	.012

TABLE A.1

May 17, 1980

Height (km)	Peak Reflectivity (dBZ)	Peak Gust Speed (m/s)	Distance between Peak Gust Speed and Environmental Wind (km)	Width of Reflectivity Greater Than 2 dBZ (km)	Range of Radar to Peak Gust (km)	Range From Generating Storm to Gust Front (km)	Range From Nearest 30 dBZ to Front (km)	Length (km)	Wind Shear s^{-1}
2.9	11	-23	2	5	59	6	6	60	.015
.4	11	-23	2.5	12	49	20	20	80	.011
.9	11	-23	2.5	10	47	15	15	70	.011
1.0	11	-23	3	10	48	15	15	70	.009
1.5	11	-23	2.5	10	48	15	15	70	.011
1.8	11	-23	2.5	7	47	10	10	65	.012
2.7	11	-23	2.5	5	47	10	10	60	.012
.3	11	-23	4	12	42	20	20	80	.007
.6	11	-23	4	10	42	15	15	70	.007
.9	11	-23	3	10	42	10	10	70	.010
1.7	11	-23	3	8	43	8	8	65	.010
2.4	11	-23	2	5	44	4	4	60	.015
.2	11	-23	4	10	31	20	20	75	.007
.4	11	-29	4	10	32	20	20	80	.009
.6	11	-29	4	8	29	18	18	80	.009
1.6	11	-23	3	5	31	10	10	75	.010
2.4	11	-23	3	5	33	10	10	60	.010
.1	11	-23	3	10	24	20	20	75	.010

TABLE A.1

May 17, 1980

Height (km)	Peak Reflectivity (dBZ)	Peak Gust Speed (m/s)	Distance between Peak Gust Speed and Environmental Wind (km)	Width of Reflectivity Greater Than 2 dBZ (km)	Range of Radar to Peak Gust (km)	Range From Generating Storm to Gust Front (km)	Range From Nearest 30 dBZ to Front (km)	Length (km)	Wind Shear s^{-1}
.3	11	-26	3	8	26	20	20	80	.011
.5	11	-26	3	7	25	20	20	80	.011
1.5	11	-23	4	5	26	10	10	65	.007
2.4	11	-23	4	5	25	10	10	60	.007
.4*	11	+23	4	13	51	30	10	80	.008
1.8	11	+32	3	7	52	10	7	30	.013

* The last two data points were obtained 20 minutes after the gust passed the radar site.

TABLE A.2

May 29, 1980

Height (km)	Peak Reflectivity (dBZ)	Peak Gust Speed (m/s)	Distance between Peak Gust Speed and Environmental Wind (km)	Width of Reflectivity Greater Than 2 dBZ (km)	Range of Radar to Peak Gust (km)	Range From Generating Storm to Gust Front (km)	Range From Nearest 30 dBZ to Front (km)	Length (km)	Wind Shear s^{-1}
.1	45	+23	7	17	27	0	0	75	.005
.3	45	+23	5	17	25	0	0	75	.008
.5	45	+23	4	17	25	0	0	65	.009
1.1	45	+23	3	12	09	0	0	40	.009
.1	45	+18	3	10	24	0	0	40	.008
.3	45	+18	3	12	23	0	0	40	.008
.4	45	+23	4	15	22	0	0	40	.007
.0	45	+28	4	15	34	0	0	65	.010
.2	45	+28	4	15	34	0	0	65	.010
.4	45	+28	5	15	34	0	0	70	.008
.7	45	+28	5	15	34	0	0	70	.008
.0	45	+32	5	15	33	0	0	65	.009
.2	45	+32	4.5	15	33	0	0	65	.010
.4	45	+32	3.5	15	36	0	0	70	.013
.7	45	+32	3.5	15	35	0	0	70	.013
.2	45	+32	6	20	35	0	0	70	.007
.4	45	+32	6	20	36	0	0	70	.007
.7	45	+32	6	20	36	0	0	70	.007
.7	45	+32	6	20	36	0	0	70	.007
.6	45	+32	6	20	36	0	0	70	.007

TABLE A.2

May 29, 1980

Height (km)	Peak Reflectivity (dBZ)	Peak Gust Speed (m/s)	Distance Between Peak Gust Speed and Environmental Wind (km)	Width of Reflectivity Greater Than 2 dBZ (km)	Range of Radar to Peak Gust (km)	Range From Generating Storm to Gust Front (km)	Range From Nearest 30 dBZ to Front (km)	Length (km)	Wind Shear s^{-1}
.5	45	+32	6	20	36	0	0	70	.007
.9	45	+32	6	20	36	0	0	70	.007
1.3	45	+32	5	20	25	0	0	45	.007

TABLE A.3

June 16, 1980

Height (km)	Peak Reflectivity (dBZ)	Peak Gust Speed (m/s)	Distance Between Peak Gust Speed and Environmental Wind (km)	Width of Reflectivity Greater Than 2 dBZ (km)	Range of Radar to Peak Gust (km)	Range From Generating Storm to Gust Front (km)	Range From Nearest 30 dBZ to Front (km)	Length (km)	Wind Shear s^{-1}
.1	11	-20	3	5	30	33	25	30	.007
.3	11	-20	2	3	32	33	25	30	.010
.6	11	-16	1	2.5	31	33	25	30	.016
.1	11	-23	2	5	28	33	25	30	.012
.3	11	-20	1.5	3	28	35	25	30	.013
.5	11	-20	.5	2	28	35	25	30	.040
.1	11	-23	4	5	27	35	23	30	.006
.3	11	-20	2.5	4	28	35	23	30	.008
.5	11	-20	1	2	27	35	22	30	.020
.1	11	-16	2	2.5	26	25	20	30	.008
.3	11	-20	2	3	26	25	20	30	.010
.5	11	-20	2	2.5	27	25	18	30	.010
.1	11	-20	2.5	4	25	25	16	30	.008
.3	11	-20	2	3	23	25	16	30	.010
.5	11	-20	1	2	23	25	16	30	.020
.1	11	-13	1	4	21	26	16	30	.013
.3	11	-20	2.5	4	23	26	16	30	.008
.4	11	-20	2	3	22	26	16	30	.010

TABLE A.4

April 10, 1981

Height (km)	Peak Reflectivity (dBZ)	Peak Gust Speed (m/s)	Distance between Peak Gust Speed and Environmental Wind (km)	Width of Reflectivity Greater Than 2 dBZ (km)	Range of Radar to Peak Gust (km)	Range From Generating Storm to Gust Front (km)	Range From Nearest 30 dBZ to Front (km)	Length (km)	Wind Shear s^{-1}
.5	11	+18	3	7	35	30	11	70	.011
.8	11	+18	3	4	40	33	12	70	.011
1.0	7	+18	1	3	40	33	13	60	.030
.2	7	+18	2	4	40	36	11	80	.015
.2	7	+18	2	5	42	36	11	80	.015
.5	7	+13	1	3	44	33	11	70	.024
.8	7	+23	1	3	45	33	12	65	.035
1.0	7	+18	1	2.5	45	26	13	50	.030
.3	11	+18	2	8	47	40	24	93	.014
.6	11	+18	2	8	49	48	24	70	.015
.9	11	+23	2.5	8	50	33	10	66	.013
1.1	11	+23	2.5	8	49	26	14	60	.017
.3	7	+18	2	7	45	48	17	85	.014
.6	7	+23	2	5	55	35	17	80	.018
1.0	7	+28	2	4	54	35	17	60	.021
.4	7	+23	2	6	58	40	15	80	.018
.7	7	+23	2.5	7	55	40	20	80	.014
1.1	7	+23	2	4	56	35	15	75	.018
.4	11	+23	3	10	58	50	12	92	.012
.4	11	+23	2	12	62	50	9	90	.018

TABLE A.4

April 10, 1981

Height (km)	Peak Reflectivity (dBZ)	Peak Gust Speed (m/s)	Distance between Peak Gust Speed and Environmental Wind (km)	Width of Reflectivity Greater Than 2 dBZ (km)	Range of Radar to Peak Gust (km)	Range From Generating Storm to Gust Front (km)	Range From Nearest 30 dBZ to Front (km)	Length (km)	Wind Shear s^{-1}
.7	11	+23	3	8	60	50	16	75	.012
1.1	11	+23	2	5	60	50	12	60	.018
.4	11	+23	1	6	64	45	12	80	.037
.7	7	+28	1	5	68	55	14	85	.040
1.1	7	+18	.5	4	60	16	6	30	.056
.5	7	+28	1	8	68	50	11	85	.042
.5	7	+23	1.5	8	68	50	11	85	.024
.5	7	+28	1	8	68	50	11	85	.042
.5	7	+28	1	7	69	55	12	90	.042

TABLE A.5

April 13, 1981

Height (km)	Peak Reflectivity (dBZ)	Peak Gust Speed (m/s)	Distance between Peak Gust Speed and Environmental Wind (km)	Width of Reflectivity Greater Than 2 dBZ (km)	Range of Radar to Peak Gust (km)	Range From Generating Storm to Gust Front (km)	Range From Nearest 30 dBZ to Front (km)	Length (km)	Wind Shear s^{-1}
.9	7	-13	.5	2.5	86	20	10	75	.032
1.5	7	-13	1.5	2	85	55	14	30	.011
2.1	7	-9	1	1	86	50	15	15	.013
.8	7	-23	1	4	83	70	9	70	.027
.8	7	-20	1	4	81	70	9	70	.024
.8	7	-20	1.5	4	78	75	9	70	.016
.8	7	-23	2	6	79	75	9	80	.014
1.4	7	-5	.5	2	74	60	15	55	.018
1.7	2	-23	.5	1	74	50	15	35	.049
.6	11	-20	2.5	6	72	65	10	80	.011
1.0	7	-23	2	2	64	60	12	55	.013
1.4	2	-16	.5	1.5	62	40	17	35	.038
.4	11	-20	2.5	8	55	75	12	80	.009
.7	7	-20	2.5	5	56	55	14	55	.009
1.1	7	-23	1.5	2.5	52	57	20	55	.019
1.8	2	-16	2	1	55	40	22	40	.009
.4	11	-15	2.5	8	54	75	15	80	.007
.7	11	-19	1.5	8	52	70	20	75	.015
1.1	7	-6	.5	2	55	50	25	52	.023
.4	11	-15	4	10	51	65	10	65	.004

TABLE A.5

April 13, 1981

Height (km)	Peak Reflectivity (dBZ)	Peak Gust Speed (m/s)	Distance Between Peak Gust Speed and Environmental Wind (km)	Width of Reflectivity Greater Than 2 dBZ (km)	Range of Radar to Peak Gust (km)	Range From Generating Storm to Gust Front (km)	Range From Nearest 30 dBZ to Front (km)	Length (km)	Wind Shear s^{-1}
.9	7	-13	.5	2.5	86	20	10	75	.032
1.5	7	-13	1.5	2	85	55	14	30	.011
2.1	7	-9	1	1	86	50	15	15	.013
.8	7	-23	1	4	83	70	9	70	.027
.8	7	-20	1	4	81	70	9	70	.024
.8	7	-20	1.5	4	78	75	9	70	.016
.8	7	-23	2	6	79	75	9	80	.014
1.4	7	-5	.5	2	74	60	15	55	.018
1.7	2	-23	.5	1	74	50	15	35	.049
.6	11	-20	2.5	6	72	65	16	80	.011
1.0	7	-23	2	2	64	60	12	55	.013
1.4	2	-16	.5	1.5	62	40	17	35	.038
.4	11	-20	2.5	8	55	75	12	80	.009
.7	7	-20	2.5	5	56	55	14	55	.009
1.1	7	-23	1.5	2.5	52	57	20	55	.019
1.8	2	-16	2	1	55	40	22	40	.009
.4	11	-15	2.5	8	54	75	15	80	.007
.7	11	-19	1.5	8	52	70	20	75	.015
1.1	7	-6	.5	2	55	50	25	52	.023
.4	11	-15	4	10	51	65	16	65	.004

TABLE A.5

April 13, 1981

Height (km)	Peak Reflectivity (dBZ)	Peak Gust Speed (m/s)	Distance Between Peak Gust Speed and Environmental Wind (km)	Width of Reflectivity Greater Than 2 dBZ (km)	Range of Radar to Peak Gust (km)	Range From Generating Storm to Gust Front (km)	Range From Nearest 30 dBZ to Front (km)	Length (km)	Wind Shear s^{-1}
.6	7	-15	3	8	49	52	20	52	.006
1.0	11	-6	1	2	49	45	20	40	.011
.3	11	-19	3	9	48	55	12	55	.007
.6	11	-11	2.5	9	46	55	20	55	.006
1.0	11	-6	1	2	44	55	15	52	.010
.2	11	-11	4	10	45	55	20	50	.004
.6	11	-6	3.5	8	44	50	20	48	.003
.2	11	-6	4	10	48	55	15	50	.003
.5	11	-6	2	8	42	48	20	40	.005

TABLE A.6

April 30, 1981

Height (km)	Peak Reflectivity (dBZ)	Peak Gust Speed (m/s)	Distance Between Peak Gust Speed and Environmental Wind (km)	Width of Reflectivity Greater Than 2 dBZ (km)	Range of Radar to Peak Gust (km)	Range From Generating Storm to Gust Front (km)	Range From Nearest 30 dBZ to Front (km)	Length (km)	Wind Shear s^{-1}
.3	21	+15	2.5	8	61	8	4	35	.034
.7	21	+23	2	8	61	8	4	35	.065
1.0	16	+11	1	4	56	9	6	15	.061
.6	21	+19	4	8	83	5	2	35	.027
1.0	21	+15	2.5	6	74	8	4	30	.034
1.2	16	+15	1.5	4	59	8	4	20	.056
.5	16	+19	2	6	82	6	4	35	.053
1.0	16	+23	1	6	73	6	4	30	.129
1.0	16	+19	2	4	55	8	6	20	.053
.3	16	+15	3	8	59	6	4	35	.028
.6	16	+15	1	6	58	6	4	30	.083
1.0	11	+15	.5	3	56	8	6	20	.166
.5	16	+23	4	8	76	6	4	40	.032
.6	16	+15	2.5	7	56	6	4	35	.033
1.0	16	+15	2	6	54	5	3	20	.041
.2	21	+15	4	9	58	6	4	40	.021
.6	16	+15	4	9	53	6	4	35	.021
1.0	16	+15	2	7	53	5	3	20	.041
.5	21	+15	4	10	77	5	2	45	.021
.7	21	+15	6	10	59	6	4	35	.014

TABLE A.6

April 30, 1981

Height (km)	Peak Reflectivity (dBZ)	Peak Gust Speed (m/s)	Distance between Peak Gust Speed and Environmental Wind (km)	Width of Reflectivity Greater Than 2 dBZ (km)	Range of Radar to Peak Gust (km)	Range From Generating Storm to Gust Front (km)	Range From Nearest 30 dBZ to Front (km)	Length (km)	Wind Shear s^{-1}
1.2	16	+15	5	10	59	5	2	20	.017
.6	21	+18	3	10	84	8	5	45	.033
1.0	21	+13	5	12	75	9	6	40	.014
1.2	21	+18	5	12	58	8	7	20	.020
.5	21	+18	5	12	75	15	10	50	.020
.8	21	+13	3	10	70	15	12	45	.024
1.3	21	+13	5	10	64	11	7	20	.014
.8	21	+18	3	8	84	20	15	50	.016
1.2	21	+7	1.5	6	87	16	13	45	.011
1.3	21	+7	3	6	66	10	8	20	.005
.8	21	+13	3.5	8	83	22	17	50	.007
1.2	16	+13	1	6	90	18	13	45	.026
1.3	21	+7	2.5	6	68	12	10	20	.005
.5	21	+18	4	10	79	25	18	50	.009
1.2	21	+18	4	9	87	17	13	45	.009
1.8	21	+7	.5	5	85	10	7	20	.022
.5	21	+13	3	10	80	30	25	50	.008
1.0	21	+7	2.5	7	86	25	20	45	.005
1.8	16	+7	.5	6	84	10	7	20	.022
.6	21	+23	4	10	84	31	25	50	.012

TABLE A.6

April 30, 1981

Height (km)	Peak Reflectivity (dBZ)	Peak Gust Speed (m/s)	Distance between Peak Gust Speed and Environmental Wind (km)	Width of Reflectivity Greater Than 2 dBZ (km)	Range of Radar to Peak Gust (km)	Range From Generating Storm to Gust Front (km)	Range From Nearest 30 dBZ to Front (km)	Length (km)	Wind Shear s^{-1}
1.2	21	+13	5	10	83	20	17	40	.005
1.9	16	+7	.5	4	86	10	7	15	.022
.6	21	+18	5	10	83	35	20	50	.006
1.2	21	+18	2	7	85	20	17	30	.015
.6	21	+18	5	10	84	25	20	50	.005
1.2	16	+7	1.5	5	86	13	10	22	.004
.6	21	+18	5	9	86	30	25	55	.005
1.2	16	+13	3	5	85	15	12	20	.006
.6	21	+18	3.5	8	85	32	25	55	.007
1.2	21	+13	3	8	86	10	7	20	.006
.5	21	+18	.5	10	82	25	22	50	.051
1.2	16	+13	1	4	88	14	9	15	.017
.6	21	+18	6	9	89	25	22	55	.004
1.4	11	+7	.5	3	93	10	7	15	.013
1.4	16	+13	.5	1	96	12	10	12	.023

TABLE A.7

May 9, 1981

Height (km)	Peak Reflectivity (dBZ)	Peak Gust Speed (m/s)	Distance between Peak Gust Speed and Environmental Wind (km)	Width of Reflectivity Greater Than 2 dBZ (km)	Range of Radar to Peak Gust (km)	Range From Generating Storm to Gust Front (km)	Range From Nearest 30 dBZ to Front (km)	Length (km)	Wind Shear s^{-1}
.5	11	-23	2	5	98	45	30	60	.015
1.4	11	-31	1	3	92	45	35	60	.038
2.0	11	-31	1	5	90	50	40	60	.039
2.7	11	-23	2	4	88	60	45	60	.015
.3	11	-20	1.5	6	79	65	45	70	.017
.9	11	-20	1	6	76	70	50	75	.026
1.6	11	-20	1	5	76	45	35	70	.026
2.2	11	-26	2	4	72	40	30	70	.016
2.8	11	-26	1	3	73	35	20	60	.032
.8	11	-20	3	8	63	70	65	85	.009
1.3	11	-26	5	8	66	70	65	80	.006
1.7	11	-20	3	7	59	65	60	75	.009
2.2	11	-20	2	7	59	60	55	75	.013
2.7	11	-20	2	6	58	55	50	70	.013
.1	11	-20	3	10	48	85	45	95	.009
.9	11	-20	3	12	47	85	40	95	.009
1.7	11	-20	2	15	45	85	45	90	.014
2.3	11	-20	1	12	42	85	45	70	.014
2.8	11	-20	1	10	40	80	35	50	.029

END

FILMED

DTIC